行政院國家科學委員會補助專題研究計畫成果報告

※※※※※※※※※※※※※※※※※※※※※※※※※
※　　　　　　　　　　　　　　　　　　　　　　　※
※　　旋轉載具上帶回饋之雙軸速率陀螺儀　　※
※　　　　的混沌控制與非線性分析　　　　　※
※　　　　　　　　　　　　　　　　　　　　　　　※
※※※※※※※※※※※※※※※※※※※※※※※※※

計畫類別：□個別型計畫　　□整合型計畫

計畫編號：NSC　89－2218－E－164－001－

執行期間：89 年 08 月 01 日至 90 年 07 月 31 日

計畫主持人：陳恒輝　助理教授

共同主持人：陳獻庚　助理教授

本成果報告包括以下應繳交之附件：

□赴國外出差或研習心得報告一份

□赴大陸地區出差或研習心得報告一份

□出席國際學術會議心得報告及發表之論文各一份

□國際合作研究計畫國外研究報告書一份

執行單位：修平技術學院機械工程系

中　華　民　國 九十 年 九 月 十 日

旋轉載具上帶回饋之雙軸速率陀螺儀的混沌控制與非線性分析

CONTROLLING CHAOS AND NONLINEAR DYNAMIC ANALYSIS OF A TWO-AXIS RATE GYRO WITH FEEDBACK CONTROL MOUNTED ON A SPACE VEHICLE

計畫編號：NSC 89-2218-E-164-001

執行期限：89 **年** 08 **月** 01 **日至** 90 **年** 07 **月** 31 **日**

主持人：陳恒輝 助理教授 修平技術學院機械工程系

共同主持人：陳獻庚 助理教授 修平技術學院工管系

計畫參與人員：蘇詩凱、陳供延、陳維荏 大專生研究助理 機械系

一、中文摘要

本論文將對一飛行器上的帶回饋之雙軸速率陀螺儀作詳細動力分析，此時飛行器相對於自轉軸作$\mu_Z(t)$轉動。當飛行器相對於自轉軸作穩態轉動時，利用 Routh-Hurwits **理論對此自治系統作穩定性分析，給出系統參數穩定條件。當飛行器相對於自轉軸作簡諧轉動時，這系統為參數激勵強非線性耗散系統，隨著系統參數變動下，系統呈現規則與混沌反應行為。經由相軌跡、龐加萊截面、平均功率普與李雅普若夫指數等數值模擬方法來分析系統，發現隨系統參數變化，系統存在數種不同型態的解與分歧行為如** Hopf **分歧、對稱分歧與倍週期分歧，並得到系統混沌行為。並在適當的力矩回饋控制下能有效地抑制混沌運動。**

關鍵詞：速率陀螺儀、分歧、混沌

Abstract

An analysis is presented of a two-axis rate gyro subjected to linear feedback control mounted on a space vehicle that is spinning with uncertain angular velocity $\mu_Z(t)$ about its spin of the gyro. For the autonomous case in which μ_Z is steady, the stability analysis of the system is studied by Routh-Hurwits theory. For the non-autonomous case in which μ_Z is sinusoidal function, this system is a strongly nonlinear damped system subjected to parametric excitation. By varying the amplitude of sinusoidal motion, periodic and chaotic responses of this parametrically excited nonlinear system are investigated using the numerical simulation. The results, Symmetry-breaking bifurcations, period-doubling bifurcations, and chaotic behavior of the system are observed by various numerical techniques such as phase portraits, Poincaré maps, average power spectra, and Lyapunov exponents. In addition, chaotic motions of this system can be suppressed and changed into regular motions by a suitable constant motor torque.

Keywords: Rate Gyro, Bifurcation, Chaos

二、Introduction

A number of studies over the past few decades have shown that chaotic phenomena are observed in many physical systems that possess both non-linearity and external excitation [1]. The nonlinearity of a system, through the various system parameters, exhibits a variety of nonlinear behaviors including jump phenomenon, multiple attractors, subharmonic vibrations, symmetry breaking-bifurcations, period-doubling bifurcations, crisis and chaos [2]. In addition, a symmetry-breaking bifurcation occurring before a period-doubling bifurcation, and the appearance of chaos amidst a cascade of period-doubling bifurcations have been observed in driven damped pendulums or Duffing's oscillators by MacDonald and Räty [3]. In a gyroscopic system, a single-axis rate gyro mounted on a space vehicle free to move in various ways also exhibits complex nonlinear and chaotic motions. The nonlinear nature and chaotic motion of a single-axis rate gyro were investigated by Ge[4] when the vehicle is spinning sinusoidally with respect to the spin axis of the gyro. This system is characterized by parametric excitation and exhibits complex nonlinear phenomena in the presence of sinusoidal excitation, including subharmonic vibrations, Hopf bifurcation, symmetry-breaking bifurcations, a series of period-doubling bifurcations, and chaos. In practice, chaotic motions are undesirable. Ge[5] used resonant parametric perturbations to change a chaotic motion into a regular one.

In this paper, an analysis is presented of a two-axis rate gyro subjected to linear feedback control mounted on a space vehicle that is spinning with uncertain angular velocity $\mu_Z(t)$ about the spin of the gyro. Here, Routh-Hurwits theory [6] is applied to analyze the stability of the autonomous case in which μ_Z is steady. For the non-autonomous case in which μ_Z is sinusoidal function, a number of numerical techniques are used to detect the existence of symmetry-breaking bifurcations, period-doubling bifurcations, and chaos of the parametrically excited nonlinear system. The natures of the periodic and chaotic motions are shown in phase plane diagrams, Poincaré maps and average power spectra. The qualitative bifurcation diagrams, parametric diagrams and quantitative Lyapunov exponents in parametric space are also computed to determine the values of bifurcation points as well as chaos onset. In addition, chaotic motions of this system can be suppressed and changed into regular motions by a suitable constant motor torque.

三、Numerical Simulations and Discussion

We consider the model of a two-axis rate gyro mounted on a space vehicle as shown in Fig. 1. Let X, Y, Z be a set of axes attached to the platform and ¶, ¦, ¸ be gimbal axes. The differential equations of a two-axis gyro with feedback control are

₠ + 2~₁ ₡ + *k*¯ + ~₂ ₢ + NF_1(¯,¤,²) = 0,

₣ + 2 ₁ ₢ + ₂¤ - ₃ ₡ + NF_2(¯,¤,²) = 0

where k=1, ₡=*d*¯/*d*², ₢ = *d*¤ /*d*²; NF_1(¯,¤,²) and NF_2(¯,¤,²), shown in Appendix A.

With the system parameter f varied, the system results obtained by numerical integration in the phase planes, Poincaré maps, average power spectra, bifurcations and Lyapunov exponents. Hopf bifurcation occurs when the parameter f≈15.4, the original equilibrium point becomes unstable and a period-2T stable symmetric limit cycle arises as shown in Fig.2, where T=2®/μ. A system with a symmetric nonlinear function can undergo either a symmetry-breaking bifurcation for the symmetric solution of the system or a period-doubling bifurcation for the asymmetric solution of the system. When f≈29.5, a symmetry-breaking bifurcation occurs. After this bifurcation, the original stable period-2T attractor becomes unstable, a pair of stable period-2T attractors arise and invert each other as shown in Fig.3 where f= 31.5. As the parameter f increases further across f≈32, a stable periodic orbit appears with double the period of the original orbit, thereby indicating a period-doubling (flip) bifurcation. When the parameter is increased, a cascade of flip bifurcations occurs and leads to the onset of chaos. At f≈34, the chaotic attractor abruptly disappears and a period-6T symmetric orbit appears, as shown in the phase plane and average power spectrum (Fig.2,4).

To investigate bifurcation further, a Poincaré plane was used to display the bifurcation diagram, which shows Poincaré fixed points x_p plotted against the system parameter f. The Hopf bifurcation, symmetry -breaking bifurcation, and period-doubling bifurcation are clearly shown. As the system parameter f is gradually increased through the parametric space, the bifurcation diagram obtained shows different types of bifurcations and chaos (Fig.5). The Hopf bifurcation at f≈15.4, the symmetry-breaking bifurcation at f≈29.5, and the period-doubling bifurcation at f=32, as observed earlier. To investigate the periodic and chaotic motions in the bifurcation diagram further, the phase planes, Poincaré maps, and power spectra are used. After a cascade of period-doubling bifurcations, the dual response becomes chaotic rather than periodic for f=32.5. When f=33, conjunction of the two inverse chaotic attractors creates a larger attractor. With the parameter increased, a large-amplitude chaotic motion appears in the phase plane, Poincaré map, and power spectrum as shown in Fig.6, where f=36.3. The power spectrum of a chaotic motion is a continuous board spectrum.

To confirm the chaotic dynamics, a quantitative Lyapunov-exponent spectrum was performed. The algorithm for calculating the Lyapunov exponents was developed by Wolf et al. [7]. A spectrum of the largest Lyapunov exponent as a function of the parameter f is shown in Fig.7. As one of the Lyapunov exponents is positive, the motion is characterized as chaotic. When at least one Lyapunov exponent $a_i = 0$ exists, motions are not stationary. For periodic motions, the Lyapunov exponents are non-positive and include only one zero Lyapunov exponent, while one negative exponent becomes zero when one type of periodic motion bifurcates to another.

Physically, chaos may be desirable or undesirable, depending on the application. In this case, we used a feedback constant control torque with the assistance of the Lyapunov exponent calculations to bring the system from a chaotic regime to a regular. For changing the parameter k form 0.5 to 1.5, there are the bifurcation diagram and the spectrum of the largest Lyapunov exponents a_{max} as the function of the stiffness coefficient k in Fig.8. As $a_{max} < 0$ for the suitable k, the system is periodic.

四、Conclusions

In this paper, a two-axis rate gyro with sinusoidal velocity about its spin axis Z exhibits the nonlinear characteristic of both sin, cos function and parametric excitation when the parameter is varied. For the autonomous case in which μ_Z is steady, the stability conditions were derived by the Routh-Hurwitz criterion. A variety of parametric studies were performed to analyze the behavior of periodic attractors route to chaos via distinct bifurcations by using the numerical simulations. The behaviors of a symmetry-breaking precursor to period-doubling bifurcations and a cascade of period-doubling route to chaos occurred in this system. The occurrence of the chaotic motion of the full system is also detected by calculating bifurcation diagrams, power spectral diagrams and Lyapunov exponents. In addition, we consider a suitable feedback constant force torque to suppress chaos in the system by computing Lyapunov exponents.

五、References

1. J. GUCKENHEIMER and P. HOLMES 1986 *Nonlinear Oscillations, Dynamical Systems and Bifurcation of Vector Fields*. Springer-Verlag, New York, Chaps. 4-7.
2. K. YAGASKI 1994 *Nonlinear Dynamics* **6**, 125-142. Chaos in a Pendulum with Feedback Control.
3. RÄTY J. VON BOEHM and H. M. ISOMÄKI 1984 *Physics Letters* **103A**, 289-292. Absence of Inversion-Symmetric Limit Cycles of Even Periods and the Chaotic Motion of Duffing's Oscillator.
4. Z. M. GE and H. H. CHEN 1997 *Journal of Sound and Vibration* **200(2)**, 121-137. Bifurcations and Chaotic Motions in a Rate Gyro with a Sinusoidal Velocity about the Spin Axis.
5. Z. M. GE and H. H. CHEN 1998 *Journal of Sound and Vibration* **209(5)**, 753-769. Double Degeneracy and Chaos in a Rate Gyro with Feedback Control.
6. L. MEIROVITCH 1970 *Methods of Analytical Dynamics*. McGraw-Hill, New York.
7. A. WOLF J. B. SWIFT H. L. SWINNEY and J. A. VASTANO 1985 *Physica* **16D**, 285-317. Determining Lyapunov Exponents From a Time Series.

Appendix A

$NF_1(\bar{\ },¤,^2) = -(A+B_1-C_1)(- c_2\mu_{Zt}\mu_n + (-\mu_n^2\ {}^2 s_1 + s_1 c_2^2 \mu_{Zt}^2 + 2\ c_2\mu_{Zt} \mu_n c_1)c_1)/[(A+A_1)\mu_n^2] - Hc(-\mu_n\ c_1 - s_1 c_2 \mu_{Zt} + \mu_n)/[(A+A_1)\mu_n^2] - (c_2 \times \mu_{Zt}\mu_n + s_2\mu_n\ \mu_{Zt})/\mu_n^2$

$NF_2(\bar{\ },¤,^2) = ((s_1^2\ c_2\mu_{Zt}\mu_n A_2 - k_2¤ s_1^2 - d_2\mu_n s_1^2)C_1 + (-\mu_{Zt}^2 s_2 A_2 + \mu_{Zt}\ \mu_n A_2)c_2(A+A_1) + (2C_1 s_1\ \mu_n^2 A_2 - C_1 s_1 c_2\ \mu_{Zt}\ \mu_n A_2 + (-\mu_{Zt}\ \mu_n \times A_2 + \mu_{Zt}^2 s_2 A_2)c_2 C_1 c_1)c_1 + (\ \mu_n C_1 s_1^2 + \ \mu_n A_2 + (s_2\mu_{Zt} A_2 - \ \mu_n A_2)c_1) \times Hc + (k_2¤ + (-s_1^2\ \mu_{Zt}\mu_n A_2 + s_1^2 s_2 \mu_{Zt}\ {}^2 A_2)c_2 + d_2\mu_n + C_1 s_1^2\ c_2 \times \mu_{Zt} \mu_n + (-\mu_{Zt}^2 s_2 + \mu_{Zt}\ \mu_n)c_2(A+A_1) + (-2s_1\ \mu_n^2 A_2 + 2C_1 s_1\ \mu_n^2 + (s_1 c_2 \mu_n A_2 - C_1 \times s_1 c_2 \mu_n)\ \mu_{Zt} + (-k_2¤ + c_2\mu_{Zt}\ \mu_n A_2 - d_2\mu_n + (\mu_{Zt}^2 \times s_2 - \mu_{Zt}\ \mu_n)c_2 C_1)c_1)c_1 + (s_2\mu_{Zt}\ \mu_n + c_1\ \mu_n)c_1 Hc + ((s_1^2 s_2 \mu_{Zt}^2 - s_1^2\ \mu_{Zt}\ \mu_n)c_2 + (-2s_1\ \mu_n^2 + s_1 c_2\ \mu_Z\ \mu_n + c_2\mu_{Zt}\ \mu_n c_1)c_1)(A + B_1))(A+B_1))/[((A+B_1)c_1^2 + C_1 s_1^2 + A_2)(A+B_1+A_2)\mu_n^2]$

where $s_1 = sin\bar{\ }$, $s_2 = sin¤$, $c_1 = cos\bar{\ }$, $c_2 = cos¤$, etc. $\mu_{Zt} = f\sin\mu^2$, $\mu = \mu_f/\mu_n$, $= d\mu_{Zt}/d^2$.

Fig.1 A two-axis rate gyro.

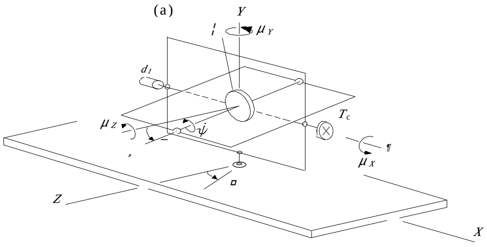

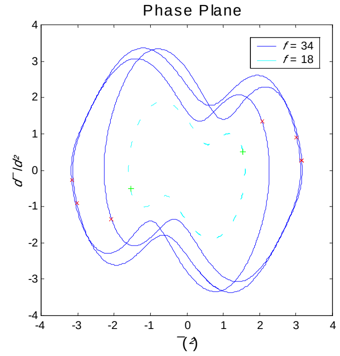

Fig.2 Two inversion-symmetric attractors: a period-2T attractor for f=18, a period-6T attractor for f= 34 where the symbols '+' and '×' indicate one period-T of $\mu_Z = f\sin\mu^2$.

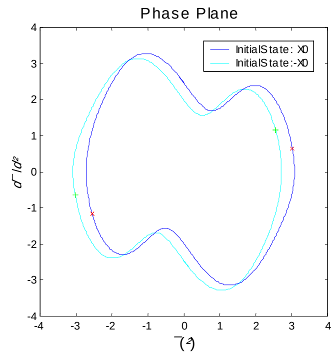

Fig.3 A dual period-2T attractor for f=31.5.

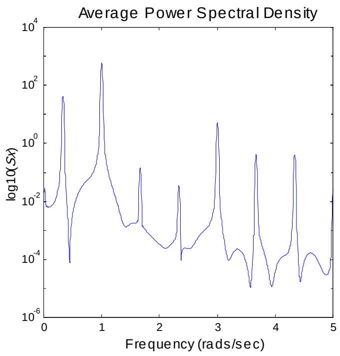

Fig.4 An average power spectrum of Fig. 4 for f=34.

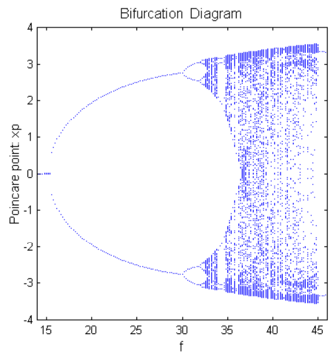

Fig.5 The bifurcation diagram.

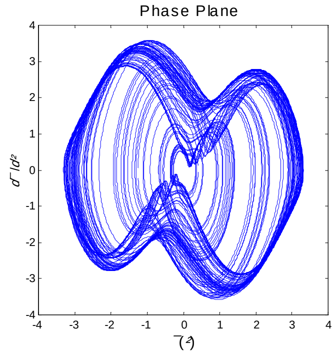

Fig.6(a) A symmetric chaotic attractor for f=36.3.

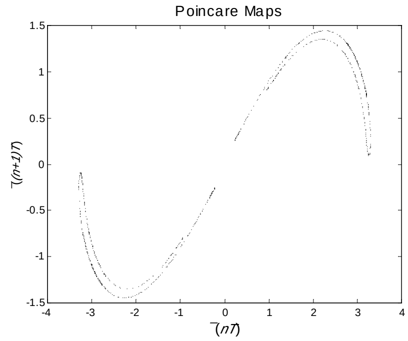

Fig.6(b) A symmetric chaotic attractor for f=36.3.

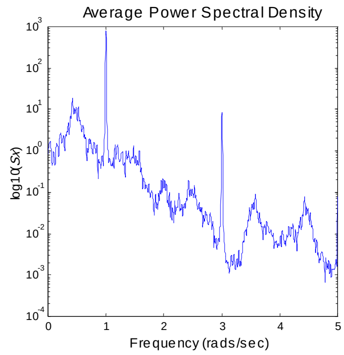

Fig.6(c) An Average power spectrum for f=36.3.

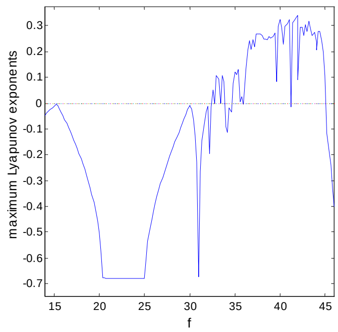

Fig.7 The largest Lyapunov exponents.

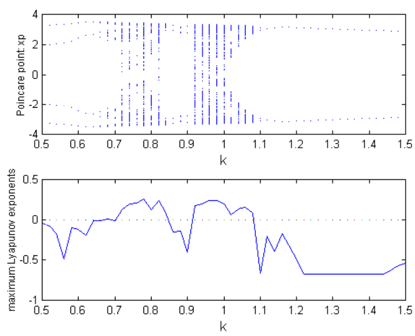

Fig.8 The bifurcation diagram and the largest Lyapunov exponent as a function of k.